Version from February 5, 2008

High-Mass Starless Cores

T.K. Sridharan[1,4], H. Beuther[1,4], M. Saito[2,4], F. Wyrowski[3,4], P. Schilke[3,4]

ABSTRACT

We report the identification of a sample of potential High-Mass Starless Cores (HMSCs). The cores were discovered by comparing images of the fields containing candidate High-Mass Protostellar Objects (HMPOs) at 1.2mm and mid-infrared (8.3μm; MIR) wavelengths. While the HMPOs are detected at both wavelengths, several cores emitting at 1.2mm in the same fields show absorption or no emission at the MIR wavelength. We argue that the absorption is caused by cold dust. The estimated masses of a few $10^2 M_\odot$ - $10^3 M_\odot$ and the lack of IR emission suggests that they may be massive cold cores in a pre-stellar phase, which could presumably form massive stars eventually. Ammonia (1,1) and (2,2) observations of the cores indicate smaller velocity dispersions and lower rotation temperatures compared to HMPOs and UCHII regions suggesting a quiescent pre-stellar stage. We propose that these newly discovered cores are good candidates for the HMSC stage in high-mass star-formation. This sample of cores will allow us to study the high-mass star and cluster formation processes at the earliest evolutionary stages.

Subject headings: stars: formation – stars: massive – ISM: dust – ISM: clouds

1. Introduction

The area of high-mass star-formation is witnessing significant progress. Systematic studies have uncovered several High-Mass Proto-Stellar objects (HMPOs) in a pre-Ultra

[1]Harvard-Smithsonian Center for Astrophysics, 60 Garden Street, MS 78, Cambridge, MA 02138, USA.

[2]National Astronomical Observatory of Japan, 2-21-1 Osawa, Mitaka, Tokyo, 181-8588, Japan

[3]Max-Planck-Institut für Radioastronomie, Auf dem Hügel 69, 53121 Bonn, Germany

[4]emails: tksridha@cfa.harvard.edu, hbuether@cfa.harvard.edu, Masao.Saito@nao.ac.jp, schilke@mpifr-bonn.mpg.de, wyrowski@mpifr-bonn.mpg.de

Compact HII (UCHII) region phase (Molinari et al 1996,2002; Sridharan et al 2002; Beuther et al 2002a). The ubiquity of the outflows in these objects points to essential similarities between the high- and the low-mass star-formation processes viz., the presence of a disk-accretion phase (Zhang et al 2005; Beuther et al 2002b). However, the characteristics of the High-Mass Starless Core (HMSC) stage which must precede the HMPO stage has barely been studied (Evans et al 2002). In contrast, recent studies of low-mass starless cores have begun to constrain the initial conditions for low-mass star-formation (Motte et al 1998; Bacmann et al 2000; Alves, Lada & Lada, 2001; Harvey et al, 2003). Similar studies of HMSCs are important in answering one of the central questions in star-formation: how do star-formation processes produce the stellar Initial Mass Function? Since high-mass stars form in clusters, and a major fraction of all stars form in such environments, the structure of the HMSCs represents the initial conditions relevant for star-formation in general.

In this letter, we present and study a sample of potential HMSCs identified by combining images at millimetre and mid-infrared wavelengths of HMPO fields. The candidate HMSCs belong to the general class of infrared-dark clouds (IRDCs), studied recently by others (Perault et al 1996; Egan et al 1998; Carey et al 2000, Bacmann et al 2000; Teyssier, Hennebelle & Perault 2002, Garay et al 2004). At the outset, we want to clarify two points: we use the terms *starless* and *pre-stellar* to indicate the lack of massive star-formation ($\gtrsim$ 8 $M_\odot$; spectral types B2 or earlier); the objects discussed here are *candidates* for the HMSC stage although this is not mentioned every time for brevity.

2. Source Sample

The data used to identify the HMSCs consist of continuum images at 1.2mm and 8.3μm wavelengths, of a sample of 69 HMPOs we have been studying (Sridharan et al 2002, Beuther et al 2002a,b, Williams, Fuller & Sridharan, 2004, 2005). The 1.2mm images obtained with the MAMBO array at the IRAM 30M telescope have been described in detail by Beuther et al (2002a). The 8.3μm images are the archival data from the Mid-Course Space Experiment (MSX; Egan et al 1998), available at the MSX web site (http://www.ipac.caltech.edu/ipac/msx/msx.html).

The 1.2mm images, each covering a $\sim 5' \times 5'$ field around an HMPO, detected multiple sources in a number of fields with an average multiplicity rate of 2.2 (Beuther et al 2002). We argued in Sridharan et al (2002) and Beuther et al (2002a) that the objects in our HMPO sample are likely to be in various stages of evolution. This is expected, given the clustered mode in which high-mass star-formation is thought to occur. Further, it is conceivable that an earlier starless stage in the high-mass star-formation process should occur in the same

fields. With this motivation, we compared the 1.2mm and the MSX A band (8.3μm) images of the HMPO fields. Strong emission at the two wavelengths was found to be typical of the HMPOs, within reasonable position uncertainties. Significant position offsets between MSX and mm emission are accounted for in terms of a cluster setting and varying evolutionary stages (Sridharan et al 2002). However, in many fields, we also discovered 1.2mm emission features associated with either MSX absorption or no detectable emission. Figure 1 shows three examples. The strongest mm emission near the center of the field in Figure 1a is associated with the HMPO-IRAS18385-0512 which is also detected at 8.3μm. The mm emission feature seen to the south east of the HMPO is associated with absorption at 8.3μm. Figures 1b (HMPO-IRAS18223-1243; also studied by Garay et al 2004) and 1c present more examples, to indicate the range of morphologies, showing filamentary structures and a field of multiple cores where a stellar cluster may be forming. Following similar observations of low-mass starless cores (for example, Bacmann et al, 2000), we suggest that the absorption is caused by the same cold dust emitting at 1.2mm. The similarity of the morphologies of the emission and absorption supports this hypothesis. In the case of IRDC-18385-0512-3, shown in Figure 1a, using a temperature of 15 K (see section 3.1), and the 1.2mm flux, a mass of 344 $M_\odot$ is estimated, making it a potential High-Mass Starless Core.

We have identified a total of 56 candidate HMSCs, listed in Table 1 along with kinematic distances, 1.2mm fluxes and mass estimates. Each object is labelled with the HMPO field and the mm-emission clump number from Beuther et al (2002a). For completeness, we have included 26 prominent MSX absorption objects either lying outside the 1.2mm images or where the images are too noisy, extending the numbering. For mass estimates (30 objects), as for the HMPOs (Beuther et al 2002a, 2005; Hildebrand 1983), we used a value of 2 for the spectral index of dust emissivity β, 100 for the gas to dust ratio, 0.1 μm for grain size and 3 g cm^{-3} for grain mass density ($\kappa = 0.4$ cm^2/gm of dust), in addition to a temperature of 15K (section 3.1). In case of distance ambiguity, the near distance has been used - at the far distance MIR absorption is unlikely. As seen in the table, the cores are massive, with masses in the range of a few $10^2 M_\odot$ - $10^3 M_\odot$.

An examination of the High Resolution processed IRAS images (HIRES; Aumann, Fowler, Melnyk 1990) of the fields failed to detect any emission from dust heated by star-formation activity. Based on the Arcetri Catalog of water masers (Valdettaro et al 2001), the General Catalog of 6.7GHz methanol masers (Pestalozzi, M.R., Minier V. and Booth, R.S., 2005) and interferometric maser observations of the HMPO fields (Beuther et al 2002c), we find two cases - IRAS18102-1800-1 & IRAS18151-1208-2 - to be associated with methanol/water maser emission respectively, implying star-formation in these cores. This suggests that the cores presented here contain objects in multiple evolutionary stages. However, all these stages represent phases before the pre-UCHII/HMPO phase, containing either

low-mass young stellar objects or early pre-cursors to the HMPOs. A further implication is that the maser activity may turn on very early in the star-formation process, and a majority of the cores presented here may be in a younger phase.

3. Observations & Results

To characterize the state of the dense gas in the sample, a subset of 34 objects from Table 1 was observed with the Effelsberg 100-m telescope for NH_3 emission in Dec 2002. The (1,1) and (2,2) inversion lines were observed simultaneously in frequency switched mode with a velocity resolution of $\Delta v = 0.25\,\mathrm{kms}^{-1}$ and ~ 4 minutes of integration time per position. The system temperatures were mostly below 50 K. Both lines were detected in all the observed sources. For 18 sources with good quality spectra, rotation temperatures were derived following Ungerechts et al. (1986). For temperatures below 20 K, as here, kinetic temperatures are only marginally higher (Danby et al., 1988). Figure 2 shows an example NH_3(1,1) spectrum, for the object IRAS18385-0512-3 (whose image is shown in Figure 1a). This core has a small linewidth of 1.1 kms^{-1}.

3.1. Ammonia line-widths and temperatures

Figure 3 compares the distributions of the ammonia line widths and rotation temperatures for the HMSCs, HMPOs and UCHII regions (Sridharan et al 2002, Churchwell et al, 1990). The HMSCs exhibit a smaller line width with a median of 1.5 kms^{-1} (mean 1.6 kms^{-1}) compared to 1.9 kms^{-1} (mean 2.1kms^{-1}) for the HMPOs. This suggests smaller internal motions and therefore more quiescent conditions, supporting the pre-stellar nature of the HMSCs. The rotation temperatures indicate colder conditions in HMSCs with a median value of 16.9 K (mean 15.3) compared to 18.5 K (mean 22.5) for HMPOs, again suggesting more quiescent conditions in the HMSCs. The corresponding ammonia line widths and temperatures for UCHII regions are 3 kms^{-1} and 22 K (Churchwell et al 1990). Thsese results support the picture where the objects evolve from HMSCs to HMPOs to UC-HII regions.

Although the ammonia rotation temperatures for the HMSCs are only marginally lower than for the HMPOs, where grey-body dust temperatures were estimated to be much higher (Sridharan et al, 2002), we believe that the dust in the HMSCs is cooler, and well characterized by the gas temperature. For the HMPOs, the best fits to the spatial and the spectral energy distributions at FIR and mm- wavelengths imply temperatures increasing inwards (Williams, Fuller & Sridharan, 2005). Ammonia emission traces the cooler outer regions of

the cores, leading to lower rotation temperature estimates. In contrast, for externally heated cores, as suggested here for the HMSCs, the dust temperature is expected to be similar to the gas temperature in the outer regions or may even be marginally lower (Li, Goldsmith & Menten, 2003). The lack of FIR emission towards the HMSCs - in cases where the the dominant HMPO in the field is not nearby, no emission is seen even at 60μm or 100μm wavelengths in the HIRES images - indicates the absence of dust heated by an embedded object.

The distributions of ammonia rotation temperatures and linewidths of the HMSCs and HMPOs were subjected to a Kolmogorov-Smirnov test, resulting in 0.90 and 0.62 for the probabilities that they are different. The masses of HMSCs are distributed over a similar range as the HMPOs. Virial masses estimated from ammonia line widths and 1.2mm sizes are lower, but comparable to dust derived masses, consistent with the HMSCs being in equilibrium. Because of the many uncertainties in mass estimates in both the cases, we do not make further comparisons.

As already noted, we use the term *starless* here to imply the absence of a massive star. From the IRAS flux limits, a luminosity upper limit of $\sim$100 $L_\odot$ is derived for a distance of 4 kpc, corresponding to early A spectral types ($\sim$ 2-3 $M_\odot$). Assuming a star-formation efficiency of 30%, an HMSC mass of 550 $M_\odot$ (sample median), and an IMF with power-law indices 2.3 and 1.3 for masses > 0.5 $M_\odot$ and 0.08 - 0.5 $M_\odot$ respectively (Kroupa, 2004), we estimate that one star of mass $\gtrsim$ 20 $M_\odot$ could form in an HMSC. While there is no current evidence for massive star-formation in these cores from their infrared fluxes, more sensitive seraches or studies like the Spitzer GLIMPSE survey will presumably uncover lower mass star-formation or hitherto unknown early stages of high-mass star-formation.

In summary, we have identified a sample of candidate high-mass starless cores, likely to contain objects in multiple stages of evolution prior to the formation of massive stars. The sample provides an opportunity to determine initial conditions for high-mass star/cluster formation and star-formation in general. The study of their internal structure at multiple wavelengths using instruments like the Sub-millimeter Array (SMA) and the Spitzer telescope will pave the way for the understanding the origin of the stellar Initial Mass Function (IMF), a central puzzle in star-formation.

H.B. thanks the Emmy-Noether-Program of the Deutsche Forschungsgemeinschaft for financial support (DFG, grant BE2578/1).

REFERENCES

Alves, J. F., Lada, C. J., Lada, E. A., 2001, Nature, 409, 159

Aumann, H. H., Fowler, J. W., & Melnyk, M. 1990, AJ, 99, 1674

Bacmann, A., Andre, P., Puget, J.-L., Abergel, A., Bontemps, S., Ward-Thompson, D., 2000, A&A, 361, 555

Beuther H., Schilke P., Menten K.M ., Motte, F., Sridharan T.K., Wyrowski F., 2002a, ApJ,566,945.

Beuther H., Schilke P., Menten K.M ., Motte, F., Sridharan T.K., Wyrowski F., 2005, ApJ, in press (Erratum).

Beuther, H., Schilke, P., Sridharan, T. K., Menten, K. M., Walmsley, C. M., Wyrowski, F., 2002, A&A, 383, 892.

Beuther, H., Walsh, A., Schilke, P., Sridharan, T. K., Menten, K. M., & Wyrowski, F. 2002c, A&A, 390, 289

Carey, S., Feldman, R., Redman, R., Egan, M., Macleod, J., Price, S., 2000, ApJ, L157

Churchwell, E., Walmsley, C. M., & Cesaroni, R. 1990, A&AS, 83, 119

Danby, G., Flower, D. R., Valiron, P., Schilke, P., & Walmsley, C. M. 1988, MNRAS, 235, 229

Egan, M. P., Shipman, R. F., Price, S. D., Carey, S. J., Clark, F. O., & Cohen, M. 1998, ApJ, 494, L199

Evans, N. J., Shirley, Y. L., Mueller, K. E., & Knez, C. 2002, ASP Conf. Ser. 267: Hot Star Workshop III: The Earliest Phases of Massive Star Birth, 267, 17

Harvey, D. W. A., Wilner, D. J., Lada, C. J., Myers, P. C., Alves, J. F., 2003, ApJ, 598, 1112

Garay, G., Faundez, S., Mardones, D. et al 2004, ApJ, 610, 313.

Kroupa, P. 2004, New Astronomy Review, 48, 47

Li, D., Goldsmith, P. F., & Menten, K. 2003, ApJ, 587, 262

Molinari, S., Brand, J., Cesaroni, R., Palla, F., 1996, A&A, 308, 573.

Molinari, S, Testi, L, Rodriguez, L. F., Zhang, Q., 2002, ApJ, 570, 758.

Motte, F., Andre, P., Neri, R., 1998, A&A, 336, 150.

Pestalozzi, M. R., Minier, V., & Booth, R. S. 2005, A&A, 432, 737

Perault, M., Omont, A., Simon, G., 1996, A&A, 315, l165

Sridharan, T. K., Beuther, H., Schilke, P., Menten, K. M., Wyrowski, F., 2002, ApJ, 566, 931.

Williams, S. J., Fuller, G. A., & Sridharan, T. K. 2005, A&A, 434, 257

Williams, S. J., Fuller, G. A., & Sridharan, T. K. 2004, A&A, 417, 115

Teyssier, D., Hennebelle, P., Perault, M., 2002, 382, 624

Ungerechts, H., Winnewisser, G., & Walmsley, C. M. 1986, A&A, 157, 207

Zhang, Q., Hunter, T. R., Brand, J., Sridharan, T. K., Cesaroni, R., Molinari, S., Wang, J., & Kramer, M. 2005, ApJ, 625, 864

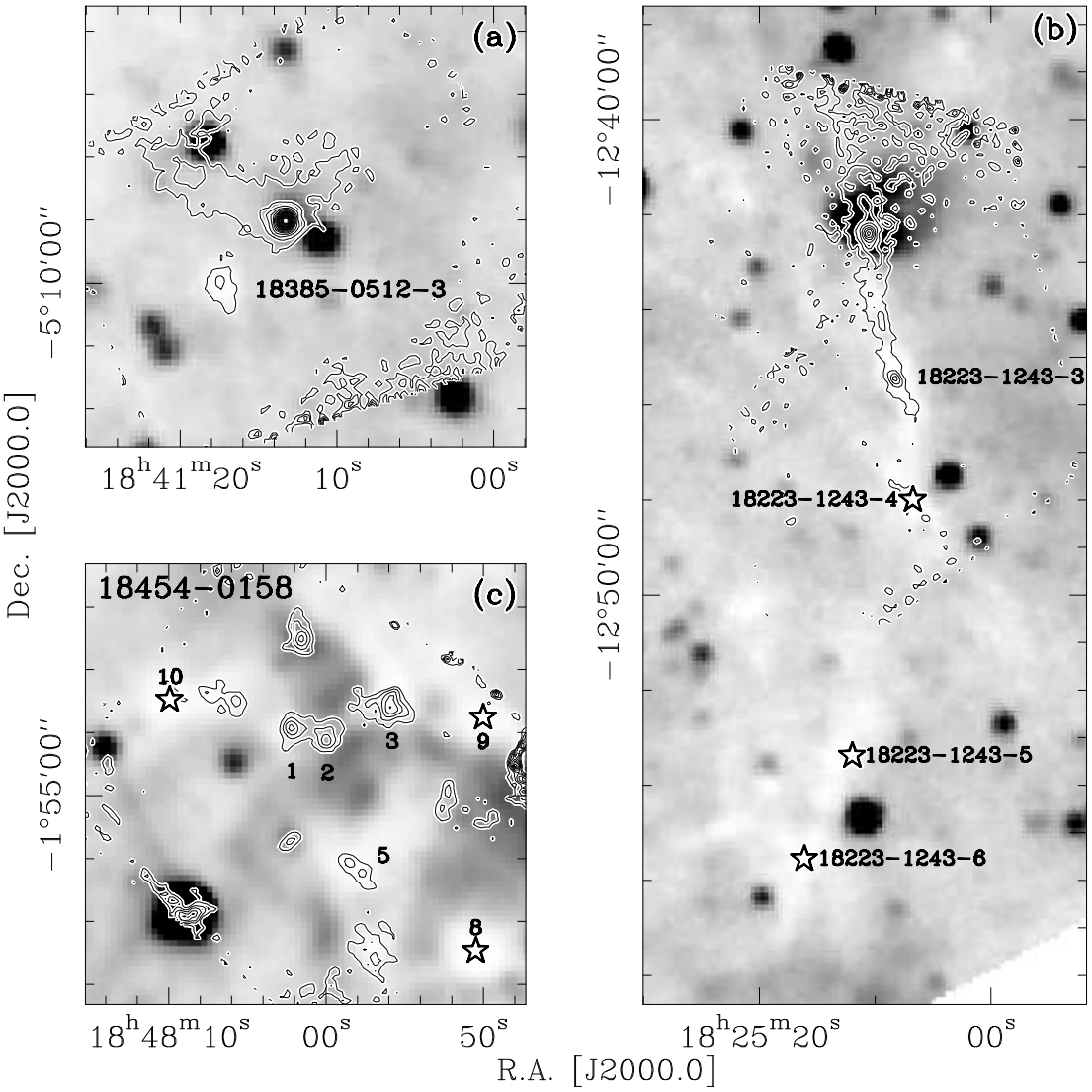

Fig. 1.— MSX A-band (8μm) images (black is bright) with 1.2mm emission contours: (a) IRDC-18385-0512-3; (b) and (c) show fields 18223-1243 and 18454-0158 with filaments and multiple cores. The star symbols mark cores lacking good 1.2mm measurements.

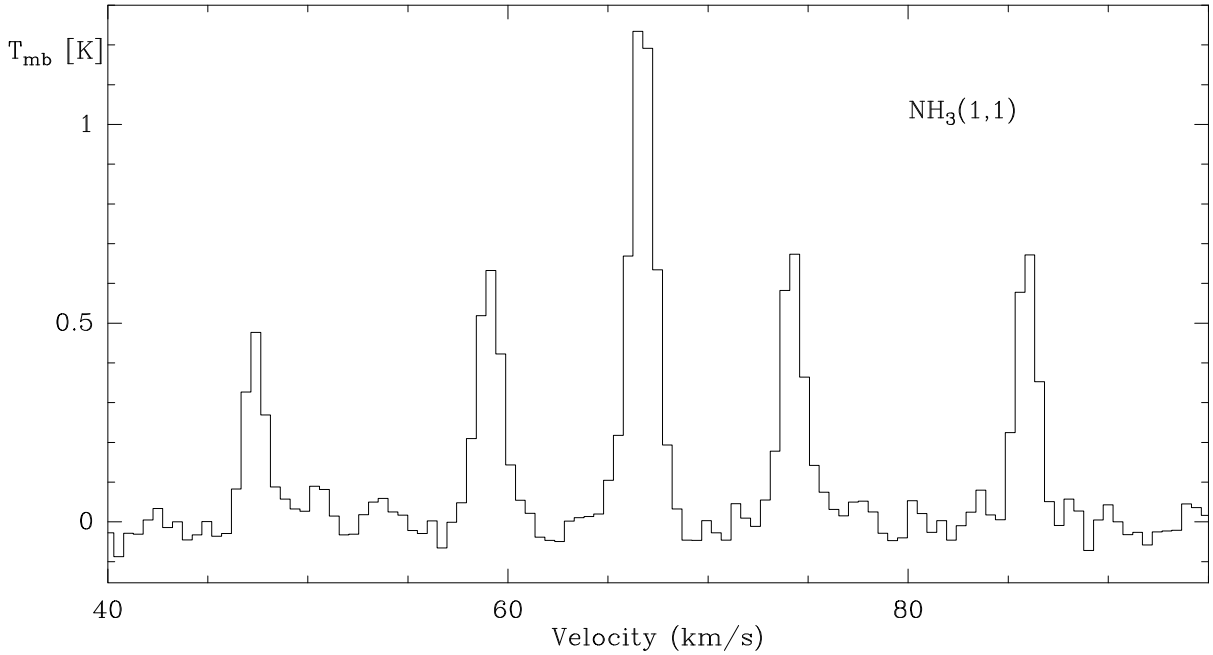

Fig. 2.— An $NH_3(1,1)$ spectrum for IRAS18385-0512-3.

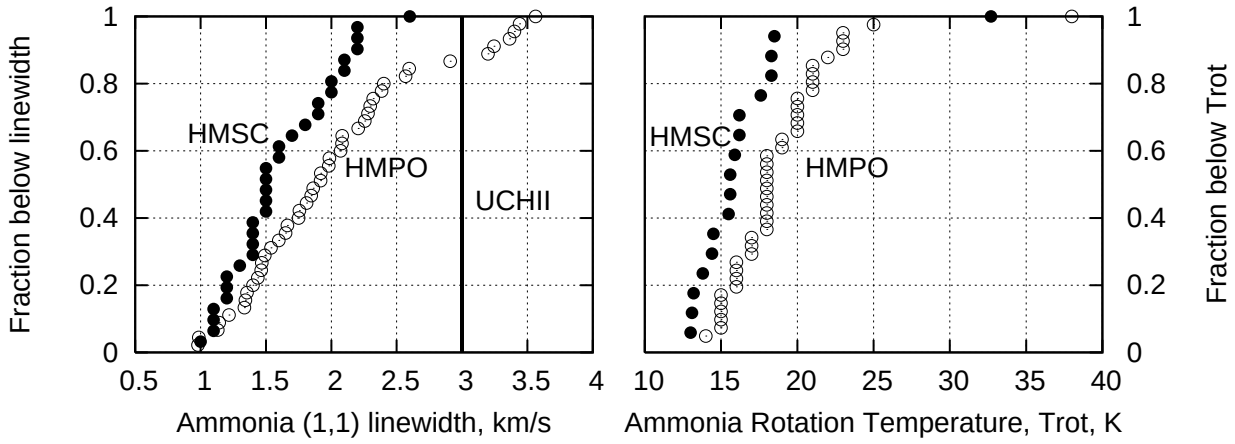

Fig. 3.— The cumulative distributions of $NH_3(1,1)$ line widhts for HMSCs and HMPOs with the median for UCHII regions shown as a vertical line (*left*). The cumulative distributions of NH_3 rotation temperatures for HMSCs and HMPOs (*right*).

Table 1. Table 1 – Candidate High-Mass Starless Cores

No	Name - Field−object#	ra	dec	D	$S_{1.3}$	v_{lsr}	Δv	T	M_{15K}
		J2000.0		kpc	Jy	km/s	km/s	K	$M_\odot$
01	IRDC-IRAS18089−1732-3	18 11 45.3	−17 30 38	3.6	0.3	34.1	2.2	15.6	241
02	IRDC-IRAS18090−1832-2	18 12 02.0	−18 31 27	6.6	0.2				541
03	IRDC-IRAS18102−1800-1	18 13 11.0	−18 00 23	2.6	3.3	14.0			1385
04	IRDC-IRAS18151−1208-2	18 17 50.3	−12 07 54	3.0	2.6	29.3	2.2	18.5	1453
05	IRDC-IRAS18182−1433-2	18 21 14.9	−14 33 06	3.6[a]	0.3	40.5	1.4	15.5	241
06	IRDC-IRAS18182−1433-3	18 21 17.5	−14 29 43			59.4	1.2		
07	IRDC-IRAS18182−1433-4	18 21 14.0	−14 34 20						
08	IRDC-IRAS18223−1243-2	18 25 10.0	−12 44 00	3.7	0.6				510
09	IRDC-IRAS18223−1243-3	18 25 08.3	−12 45 27	3.7	0.8	45.3	2.2	32.7	245[b]
10	IRDC-IRAS18223−1243-4	18 25 06.8	−12 48 00	3.7	0.3	45.4	1.4	13.0	255
11	IRDC-IRAS18223−1243-5	18 25 12.0	−12 53 23			44.7	1.1		
12	IRDC-IRAS18223−1243-6	18 25 16.2	−12 55 33			45.3/50.5	1.4/2.1		
13	IRDC-IRAS18247−1147-3	18 27 31.0	−11 44 46	6.7	0.4				1115
14	IRDC-IRAS18264−1152-2	18 29 21.0	−11 51 55						
15	IRDC-IRAS18264−1152-3	18 29 27.0	−11 50 58						
16	IRDC-IRAS18306−0835-3	18 33 32.1	−08 32 28	2.5[a]	0.8	31.6	1.6	13.1	310
17	IRDC-IRAS18306−0835-4	18 33 34.8	−08 31 20			32.1	2.0		
18	IRDC-IRAS18308−0841-2	18 33 34.3	−08 38 42	4.9	0.6				895
19	IRDC-IRAS18308−0841-3	18 33 29.3	−08 38 17	4.9	0.7	73.7	1.9	16.2	1044
20	IRDC-IRAS18308−0841-5	18 33 34.4	−08 37 36	4.9	0.2	76.7	1.5	14.5	298
21	IRDC-IRAS18308−0841-6	18 33 34.9	−08 36 04			76.9	1.6		
22	IRDC-IRAS18310−0825-4	18 33 39.5	−08 21 10	5.2	0.5	86.5	1.7	18.3	840
23	IRDC-IRAS18337−0743-3	18 36 18.2	−07 41 00	4.0	0.3	55.6	1.8	15.6	298
24	IRDC-IRAS18337−0743-4	18 36 29.9	−07 42 05			55.2	2.1		
25	IRDC-IRAS18337−0743-5	18 36 41.0	−07 39 56						
26	IRDC-IRAS18337−0743-6	18 36 36.0	−07 42 17						
27	IRDC-IRAS18337−0743-7	18 36 19.0	−07 41 48						
28	IRDC-IRAS18348−0616-8	18 37 14.7	−06 17 25			109.2			
29	IRDC-IRAS18348−0616-2[c]	18 37 27.6	−06 14 08	6.3	0.5				1232
30	IRDC-IRAS18385−0512-3	18 41 17.4	−05 10 03	4.3[a]	0.3	66.7	1.1	14.4	344
31	IRDC-IRAS18431−0312-3	18 45 45.0	−03 08 56						
32	IRDC-IRAS18431−0312-4	18 45 53.0	−03 09 01						
33	IRDC-IRAS18437−0216-3	18 46 21.9	−02 12 24	6.6[d]	0.3	110.2/96.4	1.4/1.24	15.9/13.8	811
34	IRDC-IRAS18437−0216-7	18 46 22.0	−02 14 10						
35	IRDC-IRAS18440−0148-2	18 46 31.0	−01 47 08						
36	IRDC-IRAS18445−0222-4	18 47 14.6	−02 15 44			88.2	1.0		

Table 1—Continued

No	Name - Field−object#	ra	dec	D	$S_{1.3}$	v_{lsr}	Δv	T	M_{15K}
		J2000.0		kpc	Jy	km/s	km/s	K	$M_\odot$
37	IRDC-IRAS18447−0229-3	18 47 42.0	−02 25 12			101.0	1.1		
38	IRDC-IRAS18447−0229-4	18 47 38.9	−02 28 00			98.6/111.8	1.3		
39	IRDC-IRAS18447−0229-5	18 47 31.4	−02 26 46			104.0	1.2		
40	IRDC-IRAS18454−0158-1	18 48 02.1	−01 53 56	4.7[d]	0.4	51.9/99.6	1.5/1.9		549
41	IRDC-IRAS18454−0158-3	18 47 55.8	−01 53 34	6.0[a]	0.7	93.7/97.6			1565
42	IRDC-IRAS18454−0158-5	18 47 58.1	−01 56 10	6.0[a]	0.3	93.9	1.5	17.6	671
43	IRDC-IRAS18454−0158-8	18 47 50.5	−01 57 28			94.6			
44	IRDC-IRAS18454−0158-9	18 47 50.0	−01 53 46			95.6/101.8			
45	IRDC-IRAS18454−0158-10	18 48 10.0	−01 53 29			100.4			
46	IRDC-IRAS18454−0158-11	18 48 07.0	−01 53 25						
47	IRDC-IRAS18454−0158-12	18 48 05.7	−01 53 28						
48	IRDC-IRAS18460−0307-3	18 48 36.0	−03 03 49	5.2	0.3				504
49	IRDC-IRAS18460−0307-4	18 48 46.0	−03 04 05	5.2	0.3				504
50	IRDC-IRAS18460−0307-5	18 48 47.0	−03 01 29	5.2	0.5				840
51	IRDC-IRAS18530+0215-2	18 55 29.0	+02 17 43						
52	IRDC-IRAS19175+1357-3[e]	19 19 52.1	+14 01 52	1.1[a]	0.2	7.7	1.5	15.6	15
53	IRDC-IRAS19175+1357-4[e]	19 19 50.6	+14 01 22	1.1[a]	0.2	7.7	1.5	13.2	15
54	IRDC-IRAS19410+2336-2	19 43 10.2	+23 45 04	2.1	1.4	21.4	2.0	18.3	383
55	IRDC-IRAS20081+2720-1[e]	20 10 13.0	+27 28 18	0.7	0.6	5.5			18
56	IRDC-IRAS22570+5912-3	22 58 55.1	+59 28 33	5.1	0.5	−47.1	2.6	16.2	807

[a]different velocities, kinematic distances and masses compared to those in Sridharan et al (2002) and Buether et al (2002)

[b]a dust temperature of 32.7 K was used to compute this mass; significantly higher temperature than the rest of the sample

[c]the RA reported in Beuther et al (2002) for this object is in error by ∼30”

[d]an average of the kinematic distances for the two velocity components

[e]may not qualify as high-mass; included for completeness